European Review for Medical and Pharmacological Sciences 2021; 25: 1291-1301

LncRNA DNAJC3-AS1 functions as oncogene in renal cell carcinoma *via* regulation of the miR-27a-3p/PRDM14 axis

X.-Y. NA, X.-Q. HU, Y. ZHAO, C.-H. HU, X.-S. SHANG

Department of Neurology, People's Hospital of Zhenhai District, Ningbo, China

Abstract. – OBJECTIVE: Renal cell carcinoma (RCC) is one of the most common urological malignancies worldwide. Although great advances have been made in the diagnosis and management of RCC, its prognosis remains unsatisfactory. Long noncoding RNAs (lncRNAs) have been found to be essential factors in the initiation and development of cancer. The current study aimed to measure the expression and functions of lncRNA DNAJC3-AS1 in the progression of clear cell RCC (ccRCC).

PATIENTS AND METHODS: The expression of lncRNA DNAJC3-AS1 was detected in 30 pairs of ccRCC tissues and in cell lines by RT-PCR, and its prognostic association with ccRCC was evaluated by the Kaplan-Meier method. The proliferation, migration, invasion and apoptosis of ccRCC cells were measured after silencing DNAJC3-AS1. The interaction between DNAJC3-AS1, miR-27a-3p and PRDM14 was identified by Dual-Luciferase reporter assay. The protein levels were measured by Western blotting.

RESULTS: The expression of DNAJC3-AS1 was upregulated in ccRCC tissues and cell lines compared to their normal counterparts. In vitro, silencing DNAJC3-AS1 reduced the proliferation, migration and invasion of ccRCC cells. Downregulation of DNAJC3-AS1 also led to the apoptosis of ccRCC cells. Moreover, we also found that DNAJC3-AS1 acted as a sponge of miR-27a-3p and identified PRDM14 as a target of miR-27a-3p.

CONCLUSIONS: LncRNA DNAJC3-AS1 acts as an oncogene and plays an essential role in the tumorigenesis of ccRCC, possibly via the regulation of the miR-27a-3p/PRDM14 axis.

Key Words:
Renal cell carcinoma, LncRNA DNAJC3-AS1, MiR-27a-3p, PRDM14.

Abbreviations

RCC (renal cell carcinoma); ccRCC (clear cell renal cell carcinoma); RT-PCR (real-time reverse transcription PCR); lncRNA (long non coding RNA); THOR (testis-associated highly conserved oncogenic long non-coding RNA); DNAJC3-AS1 (DNAJ/HSP40 homolog, subfamily C, member 3, anti-sense 1); RPDM14 (PR domain-containing membrane 14); SNHG12 (small nucleolar RNA host gene 12); CCK-8 (Cell Count Kit-8) ZEB1-AS1 (zinc-finger E-box binding homeobox 1, anti-sense 1); FBS (Fetal Bovine Serum); DMEM (Dulbecco's Modified Eagle's Medium); DEVD-pNA (Asp-Glu-Val-Asp-chromophore p-nitroanilide); ELISA (enzyme-linked immunosorbent assay); SDS-PAGE (sodium dodecyl sulfate-polyacrylamide gel electrophoresis); RIPA buffer (Radio-Immunoprecipitation assay buffer); PVDF (Polyvinylidene fluoride).

Introduction

Renal cell carcinoma (RCC) is a common kidney carcinoma that accounts for 80-90% of adult renal malignant tumors[1]. Worldwide, approximately 270,000 new cases of RCC are diagnosed and over ten thousand RCC patients die each year[2]. Clear cell RCC (ccRCC) accounts for approximately 90% of all RCCs in terms of histological subtype; therefore, it is one of the most lethal urological malignancies. Currently, the diagnosis of ccRCC primarily depends on computed tomography scans and magnetic resonance imaging. Because RCC is insensitive to radiotherapy or chemotherapy, the treatment of early RCC mainly relies on surgery. Although the treatment of RCC has greatly improved in the last two decades, the prognosis of RCC remains poor. Moreover, there is still a lack of effective biomarkers for predicting clinical progression and outcome in ccRCC patients. Thus, it is urgent to identify effective biomarkers and unveil the molecular mechanisms of ccRCC progression.

In recent years, long noncoding RNA (lncRNA), which was initially considered the "junk" of the genome, has been found to play an essential role in various biological activities[3]. Some stu-

Corresponding Author: Shang Xiaosong, MD; e-mail: shangxs320@163.com

dies[4-6] have shown that lncRNAs are associated with the development of various cancers, such as lung cancer, breast cancer, colorectal cancer and gastric cancer. It has been reported that various lncRNAs are involved in the tumorigenesis of RCC. For instance, lncRNA THOR is upregulated in RCC tissues and cell lines. Silencing of THOR inhibited the growth, migration and invasion of RCC cells[7]. LncRNA SNHG12 was also overexpressed in ccRCC tissues and cell lines. Inhibition of SNHG12 repressed the viability and mobility of ccRCC cells[8].

Notably, antisense partners of protein-coding genes are one type of lncRNA; these include DLX6-AS1, ZEB1-AS1 and TP73-AS1[9-11]. LncRNA DNAJC3-AS1 is a relatively novel lncRNA that is located on chromosome 13q32.1 and has 2 exons. DNAJC3, also known as P58, belongs to the heat shock protein family, which is a very conserved protein that is widely expressed in human and animal cells[12]. It is well documented that DNAJC3 can provide protective effects against various kinds of damage in cells[12,13]. However, there is little investigation about the role of DNAJC3-AS1 in ccRCC.

In the present study, the correlation between DNAJC3-AS1 and clinical data in RCC patients was investigated. Furthermore, we studied the *in vitro* effects of DNAJC3-AS1 on ccRCC cells and elucidated its underlying mechanisms.

Patients and Methods

Patients and Tissues Collection

In total, 30 pairs of ccRCC and adjacent normal tissues were collected during nephrectomy of ccRCC patients who did not receive any preoperative treatment at the hospital. The inclusion criteria were as follows: no history of other malignant tumors, no history of anticancer therapy, pathologically proven ccRCC and radical or partial nephrectomy as the treatment. The exclusion criteria were as follows: mixed histological type of primary renal cancer, larger area of necrosis and hemorrhage influencing the collection of representative area in samples, and death of the patient within the first month after surgery. The diagnosis was histologically and pathologically confirmed by 2 experienced pathologists. All tumors were staged according to the AJCC 7th system[14]. All samples were instantly frozen in liquid nitrogen after resection and then maintained in storage. Written informed consent was obtained from all patients. The Ethics Committee of the hospital reviewed and approved this study.

Cell Culture and Transfection

ccRCC cell lines (769-P, ACHN, Caki-1, 786-O) and a normal renal proximal tubular epithelial cell line (HK-2) were purchased from Shanghai Bank of Cells (Shanghai, China). Cells were cultured in DMEM (HyClone, South-Logan, UT, USA) supplemented with 10% FBS (fetal bovine serum, penicillin; 100 U/ml) and streptomycin (100 μg/mL; Gibco, Carlsbad, CA, USA). All cells were cultured in a humidified atmosphere of 5% CO_2 at 37°C. The siRNAs for DNAJC3-AS1 (si-DNAJC3-AS1 #1, si-DNAJC3-AS1 #2, si-DNAJC3-AS1 #3) and PRDM14 (si-PRDM14), and miR-27a-3p mimics, miR-27a-3p inhibitors, control siRNA (si-NC), and miR-NC mimics were synthesized by GenePharma Ltd (Suzhou, China). The coding region of PRDM14 was amplified from cDNA and cloned into pcDNA3.1 (pcDNA3.1 PRDM14). Transfection was performed using Lipofectamine 3000 (Life Technologies, Carlsbad, CA, USA) according to the manufacturer's instructions.

Cell Proliferation Assay

The proliferation of cells was measured by the Cell Counting Kit-8 (CCK-8; Solarbio, Beijing, China) assay according to the manufacturer's instructions. Briefly, cells were plated in 96-well culture plates at a density of 1×10^4 cells/well and cultured in fresh medium mixed with CCK-8 at a ratio of 10:1 for 2 h. The cell density was measured with a microplate reader (Biotek, Winooski, VT, USA) at 490 nm.

RNA Purification and RT-PCR

RNA was extracted from cells or tissues using TRIzol (Life Technologies, Carlsbad, CA, USA). The concentration and quality of RNA were assayed using a NanoDrop 2000 Spectrophotometer (Thermo Scientific, Waltham, MA, USA). One microgram of total RNA was reverse transcribed into cDNA using the High Capacity cDNA Reverse Transcriptase Kit (Life Technologies, Carlsbad, CA, USA). qRT-PCR was carried out using SYBR Green^{TM} qPCR SuperMix Universal (Life Technologies, Carlsbad, CA, USA) on an Applied Biosystems 7500 Detection System (Applied Biosystems, Foster City, CA, USA) to measure the expression of DNAJC3-AS1, miR-27a-3p, PRDM14, U6 and GAPDH. The following primers were used:

DNAJC3-AS1 forward: 5′-AGCGATTGTGGAAGACCCTG-3′ and reverse: 5′-ATTTCCCCTGGTAAGCGCAA-3′; miR-27a-3p forward: 5′-TTCACAGTGGCTAAGTTCCGC-3′ and 5′-AGGG CTTAGCTGCTTGTGAGCA-3′; PRDM14 forward: 5'-TGAGCCTTCAGGTCACAGAG-3' and reverse 5'-ATTTCCTATCGCCCTTGTCC-3'; U6 forward: 5′-CTCGCTTCGGCAGCACA-3′ and reverse 5′-AACGCTTCACGAATTTGCGT-3′; and GAPDH forward: 5′-GGTGAAGGTCGGAGTCAACG-3′ and reverse: 5′-CAAAGTTGTCATGGATGTACC-3′. The PCR conditions were as follows: 95°C for 10 min, 40 cycles of 95°C for 15 s, and 60°C for 60 s. PCR amplification was performed in triplicate. Changes in threshold cycle (CT) values were calculated via the CT ($2^{-\Delta\Delta CT}$) method.

Migration and Invasion Assay

To measure the migration ability of cells, a wound healing assay was applied. Briefly, transfected cells were seeded into 6-well plates and grown to confluence. Then, the monolayer cells were scratched by a sterile 200 μL pipette tip, and the wounded monolayer of cells was cultured for 24 hrs. Photographs of the center of the wound edges were randomly captured using an inverted microscope (Olympus Corporation Co. Ltd., Tokyo, Japan) at 100 × magnification. Migratory capacity was measured as the relative migratory distance. All experiments were carried out in triplicate.

Transwell assays were used to measure the invasion capacity of cells. Twenty-four-well transwell chambers (8 μm, Corning, NY, USA) were used. First, the upper chambers were precoated with 60 μl of Matrigel (BD Biosciences, Franklin Lakes, NJ, USA). Cells were seeded in the upper chambers in serum-free medium at a density of 4×10^4 cells/chamber, while the lower chamber was supplemented with full medium with 10% FBS. After incubation at 37°C for 48 h, the inserts were stained with 0.5% crystal violet (Solarbio, Beijing, China) for 30 min. The number of invaded cells was counted in random fields under an inverted microscope (Olympus Corporation Co. Ltd., Tokyo, Japan) at 100 × magnification. Invasion capacity was measured as relative cell counts. All experiments were carried out in triplicate.

Caspase-3 Activity Assay

The activity of caspase-3 was measured using a caspase-3 colorimetric assay kit (Abcam, Cambridge, MA, USA) according to the manufacturer's instructions. Briefly, the enzymatic reaction for caspase-3 activity was performed in a 96-well plate. After transfection for 24 h, cells were collected and lysed. Fifty microliters of lysates were added into each well. A 50 μl aliquot of 2× reaction buffer was added to each sample. Then, 200 μM DEVD-pNA was added as the caspase-3 substrate. The reaction mixtures were mixed and incubated at 37°C for 2 h. Then, the absorbance was measured by a microplate reader (Biotek, Winooski, VT, USA) at 405 nm.

Apoptosis Assay

The apoptosis of cells was performed with the Cell Death Detection Enzyme-linked Immunosorbent Assay (ELISA) kit (Roche, Basel, Switzerland) according to the manufacturer's instructions. Briefly, the cells were collected and lysed 24 h after transfection. Then, antibodies against single-strand DNA and histones (H1, H2a, H2b, H3 and H4) specifically bind both mononucleosomes and oligonucleosomes derived from apoptotic cells. Biotinylated anti-histone antibodies fixed the antibody-nucleosome complexes to the streptavidin-coated microtiter plate. Then, the anti-DNA antibodies were conjugated with horseradish peroxidase to generate a colored product. The addition of stop solution changed the color to yellow. The absorbance was measured by a microplate reader (Biotek, Winooski, VT, USA) at 405 nm. The rate of apoptosis was measured by assessing the enrichment of nucleosomes in the cytoplasm.

Luciferase Activity Assay

Bioinformatics methods were used to analyze the relationship between DNAJC3-AS1, miR-27a-3p and PRDM14. Predicted binding sites for miR-27a-3p in DNAJC3-AS1 and predicted binding sites for miR-27a-3p in the 3'-UTR of PRDM14 were cloned into a dual luciferase reporter vector, psi-check2, by Synbio Technologies (Suzhou, China). The constructed vectors were then transfected with miR-650 mimics using Lipofectamine 2000 (Life Technologies, Carlsbad, CA, USA). Forty-eight hours after transfection, cells were harvested, and luciferase activity was assayed using the Dual-Luciferase Reporter Assay System (Promega, Madison, WI, USA) according to the manufacturer's instructions.

Western Blot

Western blotting was performed as described previously[15]. Briefly, cells were collected and lysed in RIPA buffer (Solarbio, Beijing, China). The

total lysates were separated by 12% SDS-PAGE and transferred onto PVDF membranes (Millipore, Billerica, MA, USA). The membranes were blocked with 10% skimmed milk for 1 h at room temperature. Then, the membranes were blocked with the following primary antibodies at 4°C overnight. Bcl-2, Bcl-xl, Caspase-3, cleaved caspase-3, GAPDH (Cellular Signaling Technology, Danvers, MA, USA) PRDM14 (Abcam, Cambridge, MA, USA). Next, after washing with TBST for 10 mins, the membranes were incubated with the corresponding horseradish peroxidase-conjugated secondary antibody (goat anti-mouse, goat anti-rabbit, Sigma-Aldrich, St. Louis, MO, USA) for 1 h at room temperature. Signals were detected by a chemiluminescence kit (Thermo Fisher Scientific, Waltham, MA, USA) according to the manufacturer's instructions.

Statistical Analysis

Statistical analyses were performed with GraphPad Prism 7.0 (GraphPad Software, 2007, La Jolla, CA, USA). Data are expressed as the mean ± SD. One-way ANOVA was used to determine the significance of differences between multiple groups. A post-hoc test was used to calculate the significance of differences between two groups. A p-value <0.05 (two-tailed) was considered statistically significant.

Results

DNAJC3-AS1 Was Upregulated in ccRCC and Correlated With Poor Prognosis

First, we measured the expression of DNAJC3-AS1 *in vivo* by RT-PCR. The expression levels of DNAJC3-AS1 were higher in ccRCC tissues than in normal tissues (Figure 1A). Then, we analyzed the expression of DNAJC3-AS1 in five cell lines, namely, HK-2, 769-P, ACHN, Caki-1 and 786-O. Compared to that in the normal proximal tubular epithelial cell line (HK-2), the expression of DNAJC3-AS1 was significantly upregulated in 769-P, ACHN, Caki-1 and 786-O cell lines (Figure 1B). The expression levels of DNAJC3-AS1 were higher in Caki-1 and 786-o cells, which were chosen for further studies. In addition, Kaplan-Meier survival analysis was performed to investigate the relationship between the expression of DNAJC3-

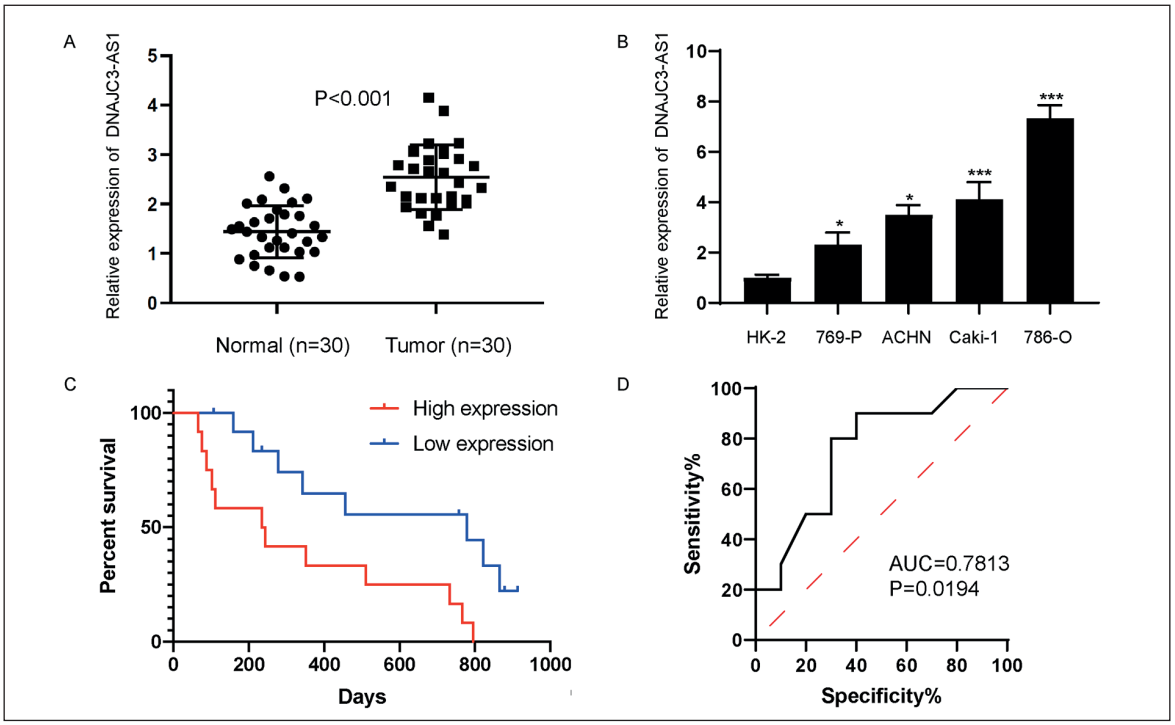

Figure 1. The expression of DNAJC3-AS1 is upregulated in ccRCC tissues and cell lines. **A,** The expression of DNAJC3-AS1 was evaluated in 30 paired ccRCC tissues and adjacent normal tissues by qRT-PCR. **B,** The expression of DNAJC3-AS1 was evaluated in HK-2, 769-P, ACHN, Caki-1 and 786-O cells. **C,** Kaplan-Meier analysis of the association between DNAJC3-AS1 expression and the survival time in ccRCC patients. **D,** Assessment of the diagnostic efficacy of DNAJC3-AS1 in ccRCC patients. Three independent experiments were performed and data shown are mean ± SD. Statistically significant differences are indicated as *, p<0.05, ***, p<0.001.

AS1 and the survival of ccRCC patients. As indicated in Figure 1C, ccRCC patients with high DNAJC3-AS1 expression had relatively short survival times, while those with low DNAJC3-AS1 expression had relatively long survival times ($p<0.05$). The correlation between the expression of DNAJC3-AS1 and the clinicopathologic features of ccRCC patients is indicated in Table I. DNAJC3-AS1 expression was correlated with tumor stage, tumor size, lymph node metastasis, distant metastasis and pathological grade but was not significantly correlated with age or sex. Then, the diagnostic efficacy of DNAJC3-AS1 was evaluated. The ROC curve analysis showed that the AUC was 0.7813 ($p<0.05$). Taken together, these data suggest that DNAJC3-AS1 is markedly upregulated in ccRCC, and its expression has clinical significance for the diagnosis of ccRCC.

Silencing of DNAJC3-AS1 Inhibited the Proliferation, Migration, and I nvasion and Triggered the Apoptosis of ccRCC Cells

Transfection of DNAJC3-AS1 siRNAs was performed to silence the expression of DNAJC3-AS1, and transfection with the 3 siRNAs successfully decreased the expression of DNAJC3-AS1 in both Caki-1 and 786-O cells compared with that in the negative control group (Figure 2A). Moreover, among those siRNAs, siRNA1 exhibited the best knockdown effect; therefore, siRNA1 was chosen for subsequent experiments investigating the biological function of DNAJC3-AS1.

First, cell proliferation was measured by CCK-8 assays after downregulation of DNAJC3-AS1. As indicated in Figure 2B, silencing of DNAJC3-AS1 led to the inhibition of cell proliferation in both 786-O and Caki-1 cells compared to that in their si-NC control groups. Then, we assayed the effects of the downregulation of DNAJC3-AS1 on the invasion and migration of cells. Transwell chamber and wound healing assays were performed. Compared with that in the si-NC group, cell invasion and migration were significantly inhibited in the DNAJC3-AS1 silencing group (Figure 2C, D). Next, we measured apoptosis after silencing DNAJC3-AS1. As indicated in Figure 2E, the apoptosis rate was significantly increased in the DNAJC3-AS1-silenced group compared with the si-NC transfection group ($p<0.001$). We also assessed apoptosis-related proteins. The protein levels of antiapoptotic proteins such as Bcl-2 and Bcl-xl were decreased, while cleaved caspase-3 was increased after silencing DNAJC3-AS1 in both Caki-1 and 786-O cells (Figure 2F). Furthermore, a caspase-3 activity assay also revealed that the activation of caspase-3 was enhanced after the downregulation of DNAJC3-AS1 (Figure 2G).

Table I. Correlation between DNAJC3-AS1 expression and clinicopathologic features.

Characteristics	N (82)	DNAJC3-AS1 expression		*p*-value
		High (%)	Low (%)	
Gender				
Female	40	16	24	0.319
Male	42	20	22	
Age (y)				
≤ 60	31	11	20	0.267
> 60	51	23	28	
Clinical Stage				
I-II	38	17	21	0.027
III-IV	44	30	14	
Tumor size				
≤ 4 cm	49	18	31	0.003
> 4 cm	33	23	10	
Lymph node metastasis				
None	47	20	27	0.008
Yes	35	25	10	
Distant metastasis				
None	22	8	14	0.004
Yes	60	43	17	
Pathological grade				
G1-G2	52	28	24	0.033
G3-G4	30	23	7	

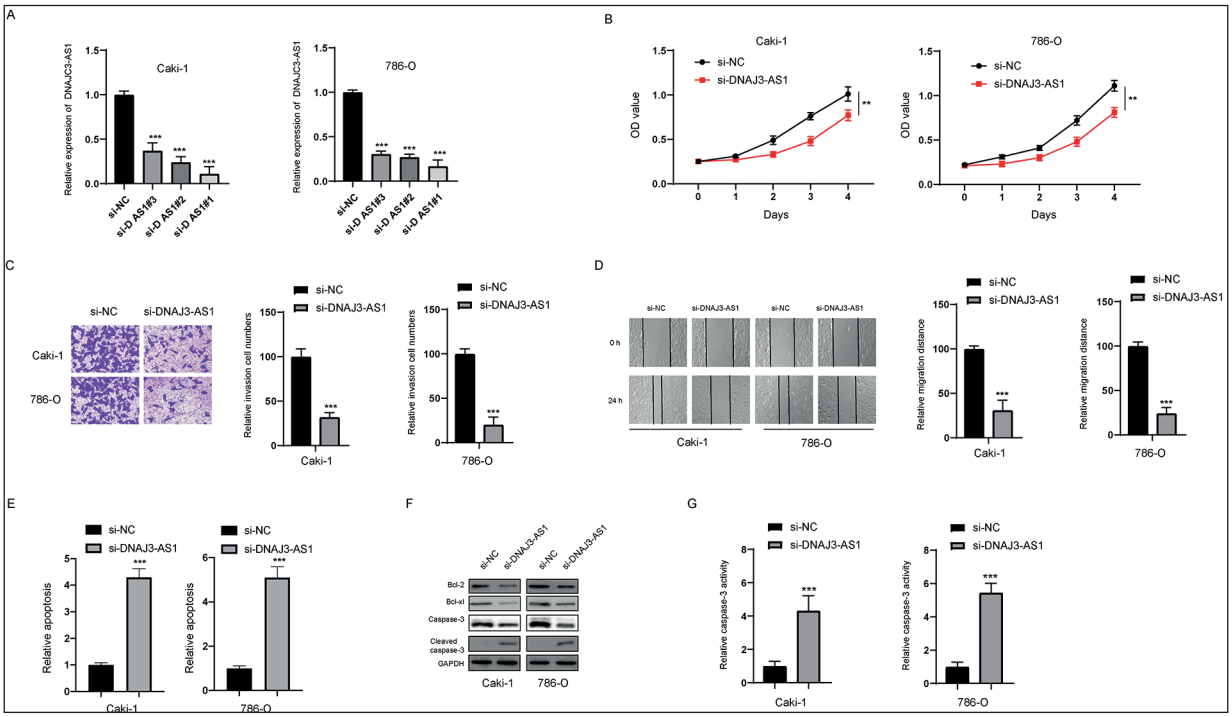

Figure 2. Silencing of DNAJC3-AS1 had effects on the biological behaviour of ccRCC cells. **A,** Caki-1 and 786-O cells were transfected with three different siRNAs against DNAJC3-AS1 for 24 h, then the expression levels of DNAJC3-AS1 were measured by RT-PCR. **B,** Cell proliferation was assayed by the CCK-8 assay after silencing of DNAJC3-AS1. **C,** Cell invasion was measured by the transwell invasion assay after knockdown of DNAJC3-AS1. **D,** Cell migration was measured by the wound healing assay after knock-down of DNAJC3-AS1. **E,** Cellular apoptosis was measured by Nucleosome apoptosis ELISA after silencing of DNAJC3-AS1. **F,** The proteins levels of apoptosis-related proteins were measured by Western blot after silencing of DNAJC3-AS1. **G,** The activity of caspase-3 was measured after silencing of DNAJC3-AS1. Three independent experiments were performed and data shown are mean ± SD. Statistically significant differences are indicated as **, $p<0.01$, ***, $p<0.001$.

DNAJC3-AS1 Functions As a ceRNA for MiR-27a-3p in ccRCC Cells

Some studies indicate that multiple lncRNAs can function as sponges to regulate the function of miRNAs. Therefore, we investigated the possibility that DNAJC3-AS1 may also function as a ceRNA. To test this hypothesis, we used a bioinformatics tool (StarBase v2.0) to predict the putative miRNA-binding sites in DNAJC3-AS1. The binding site is presented in Figure 3A. To verify this, we cotransfected the luciferase reporter plasmid DNAJC3-AS1 WT or DNAJC3-AS1 MUT with miR-NC or miR-27a-3p into Caki-1 and 786-O cells. MiR-27a-3p decreased the Luciferase activity of DNAJC3-AS1 WT but not DNAJC3-AS1 MUT (Figure 3B). Furthermore, we found that the expression of miR-27a-3p was downregulated and negatively correlated with the expression of DNAJC3-AS1 in ccRCC tissues (Figure 3C, D). To further verify the correlation of DNAJC3-AS1 and miR-27a-3p, we transfected ccRCC cells with si-DNAJC3-AS1 and miR-27a-3p inhibitors. As shown in Figure 3E, F, G, H, transfection of miR-27a-3p inhibitors reversed the effect of DNAJC3-AS1 silencing on the proliferation, invasion, migration and apoptosis of ccRCC cells. In addition, the effects of DNAJC3-AS1 silencing on apoptosis-related proteins and caspase-3 activity were abolished by miR-27a-3p inhibitors (Figure 3 I, J). Taken together, these data indicated that DNAJC3-AS1 exerts its biological functions at least partially via regulation of miR-27a-3p.

PRDM14 Is a Direct Target of MiR-27a-3p

MiRNAs usually bind with specific mRNAs to regulate the expression of target genes[16]. Bioinformatic analysis showed that PRDM14 is a potential target of miR-27a-3p, and the putative binding site between PRDM14 and miR-27a-3p is indicated in Figure 4A. We first transfected ccRCC cells with miR-NC or miR-27a-3p mimics. Both the protein and mRNA levels of

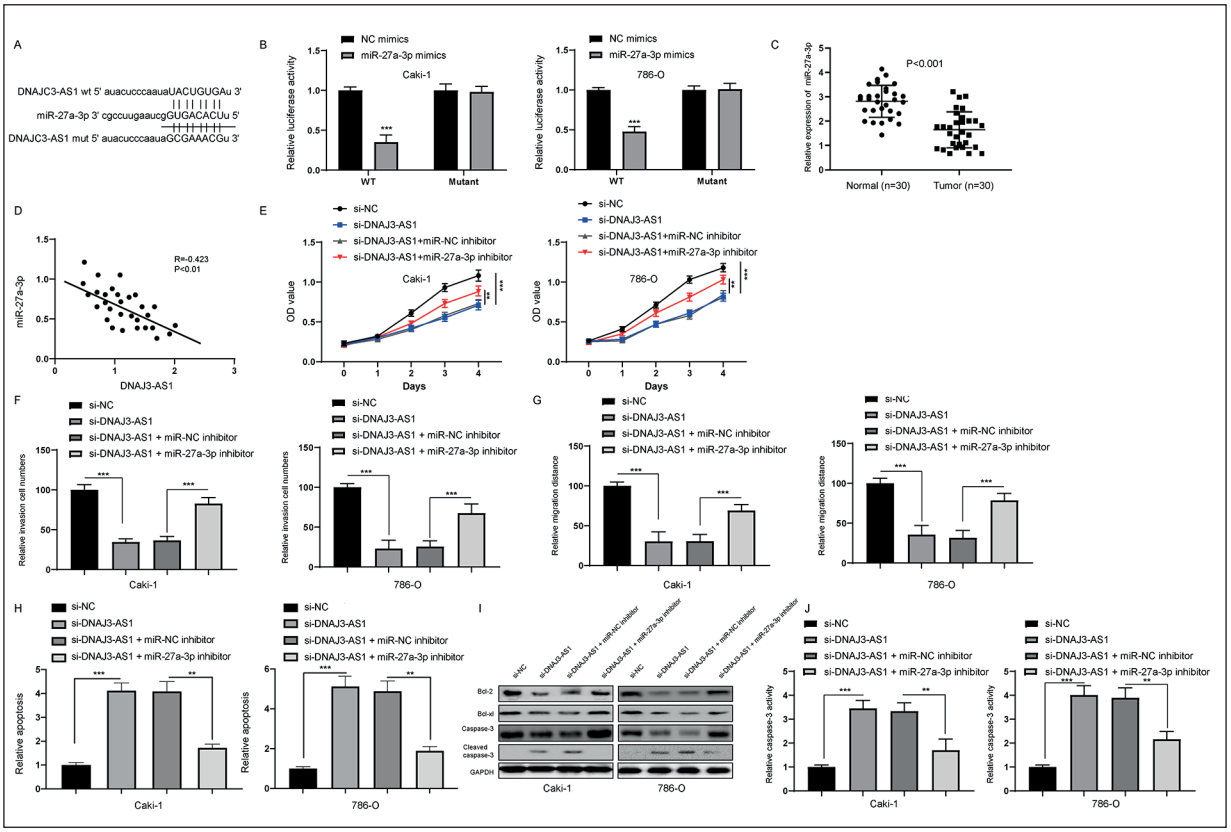

Figure 3. MiR-27a-3p is a target of DNAJC3-AS1. **A,** The prediction binding site between miR-27a-3p and DNAJC3-AS1. **B,** Luciferase reporter assay was used to test the interaction between miR-27a-3p and DNAJC3-AS1. **C,** The expression levels of miR-27a-3p was measured in 30 pairs of ccRCC and adjacent normal tissues. **D,** Pearson correlation analysis between DNAJC3-AS1 and miR-27a-3p in ccRCC tissues. **E,** Caki-1 and 786-O cells were treated as indicated, then cell proliferation was assayed by the CCK-8 assay. **F,** Caki-1 and 786-O cells were evaluated as indicated, then the invasion of cells was measured. **G,** Caki-1 and 786-O cells were treated as indicated, then the migration of cells was measured. **H,** Caki-1 and 786-O cells were treated as indicated, then the apoptosis of cells was measured. **I,** Caki-1 and 786-O cells were treated as indicated, then the apoptosis-related proteins were assessed by Western blot. **J,** Caki-1 and 786-O cells were estimated as indicated, then the caspase-3 activities were measured. Three independent experiments were performed and data shown are mean ± SD. Statistically significant differences are indicated as **, p <0.01, ***, p <0.001.

PRDM14 were significantly downregulated in the miR-27a-3p mimics transfection group compared to the control group (Figure 4B, C). We further verified that PRDM14 is a target of miR-27a-3p. Then, PRDM14 WT or PRDM14 MUT was co-transfected with miR-NC or miR-27a-3p mimics into Caki-1 and 786-O cells. Luciferase reporter assay results showed that luciferase activity was significantly decreased in the PRDM14 WT + miR-27a-3p group compared with the PRDM14 WT + miR-NC group, while the PRDM14 MUT + miR-27a-3p groups showed no difference from the PRDM14 MUT + miR-NC group, implying that PRDM14 was a target of miR-27a-3p (Figure 4D). Then, we measured the mRNA levels of PRDM14 in ccRCC tissues and adjacent normal tissues. The mRNA levels of PRDM14 were significantly upregulated in ccRCC tissues compared with normal tissues (Figure 4E). In addition, Pearson analysis showed that the expression of PRDM14 was negatively correlated with the expression of miR-27a-3p *in vivo* (Figure 4F). To unveil the function of PRDM14, we transfected ccRCC cells with siRNAs to knockdown PRDM14 (Figure 4G). We found that silencing PRDM14 inhibited the proliferation of Caki-1 and 786-O cells (Figure 4H). In addition, similar to the silencing of DNAJC3-AS1, downregulation of PRDM14 also inhibited the invasion and migration of ccRCC cells (Figure 4I, J). In addition, silencing PRDM14 also increased apoptosis, changed the expression of apoptosis-related proteins and increased the activation of caspase-3 in ccRCC cells (Figure 4

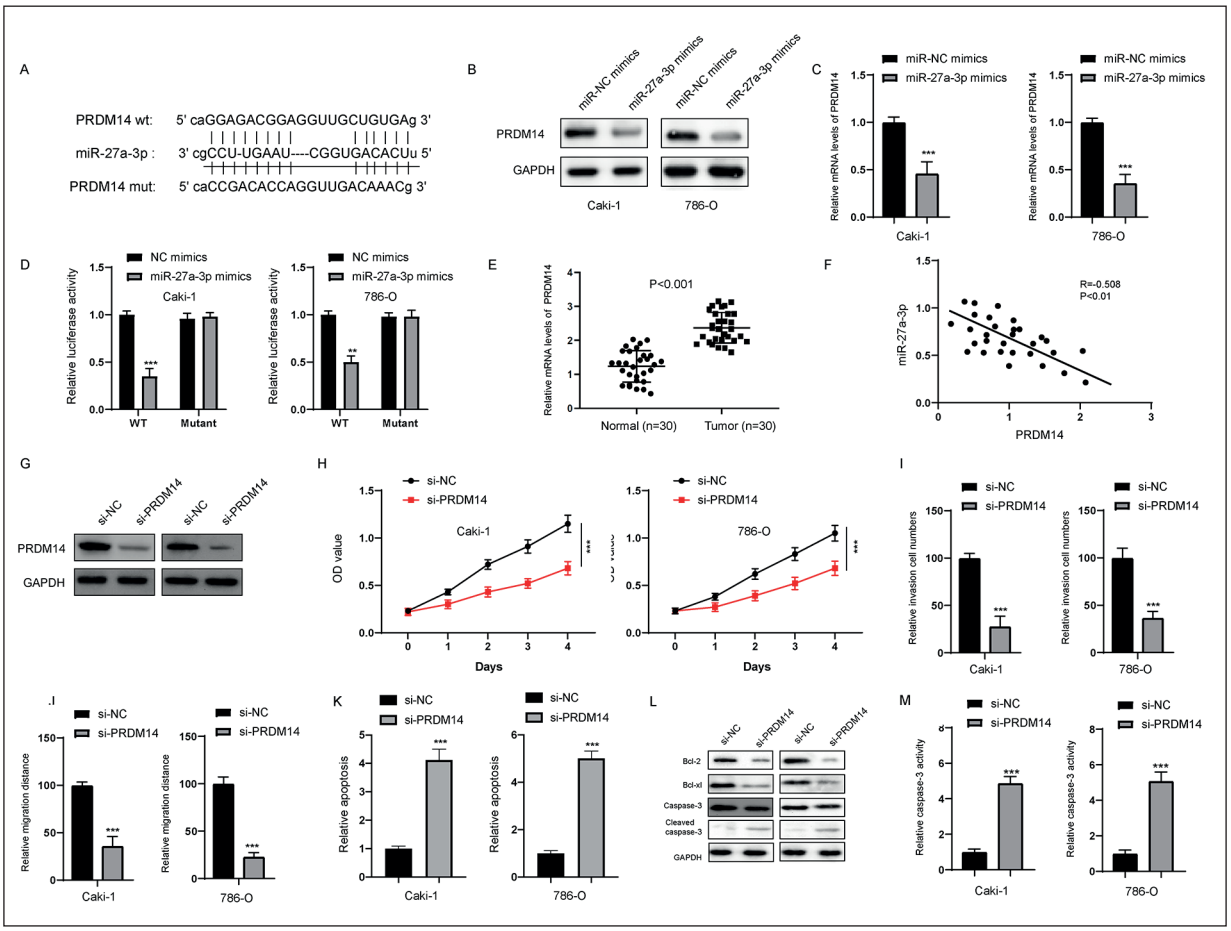

Figure 4. PRDM14 is a direct target of miR-27a-3p. **A,** The prediction binding site between miR-27a-3p and 3'UTR region of PRDM14. **B,** Caki-1 and 786-O cells were transfected with miR-NC or miR-27a-3p mimics for 24 h, then the protein levels of PRDM14 were assayed by Western blot. **C,** Caki-1 and 786-O cells were transfected with miR-NC or miR-27a-3p mimics for 24 h, then mRNA levels of PRDM14 were assayed. **D,** Luciferase reporter assay was used to test the interaction between miR-27a-3p and PRDM14. **E,** The expression of DNAJC3-AS1 was evaluated in 30 paired ccRCC tissues and adjacent normal tissues by qRT-PCR. **F,** Pearson correlation analysis between DNAJC3-AS1 and miR-27a-3p in ccRCC tissues. **G,** Caki-1 and 786-O cells were transfected with si-NC and si-PRDM14 for 24 h, then the protein levels of PRDM14 were assayed by Western blot. **H,** Caki-1 and 786-O cells were transfected with si-NC and si-PRDM14 for indicated time, then cell viabilities were assayed by CCK-8. **I,** Cell invasion was measured by the transwell invasion assay after silencing of PRDM14. **J,** Cell migration was measured by the wound healing assay after knock-down of PRDM14. **K,** Cellular apoptosis was measured by Nucleosome apoptosis ELISA after silencing of PRDM14. **L,** The proteins levels of apoptosis-related proteins were measured by Western blot after silencing of PRDM14. **M,** The activity of caspase-3 was measured after silencing of PRDM14. Three independent experiments were performed and data shown are mean ± SD. Statistically significant differences are indicated as **, $p<0.01$, ***, $p<0.001$.

K, L, M). Taken together, these data suggested that PRDM14 is a target of miR-27a-3p and that DNAJC3-AS1 might exert its effects at least partially *via* regulation of PRDM14.

Overexpression of PRDM14 Abrogated the Effects of DNAJC3-AS1 Silencing on ccRCC Cells

Then, we examined the protein levels of PRDM14 after silencing DNAJC3-AS1. As indicated in Figure 5A, silencing of DNAJC3-AS1 also led to the downregulation of PRDM14. To further analyze the relationship between PRDM14 and DNAJC3-AS1, we forced the expression of PRDM14 in ccRCC cells *via* transfection of pcDNA3.1 PRDM14 (Figure 5B). CCK-8 assay results showed that the inhibition of proliferation caused by silencing DNAJC3-AS1 was significantly rescued by overexpression of PRDM14 (Figure 5C). In addition, the effects of silencing DNAJC3-AS1

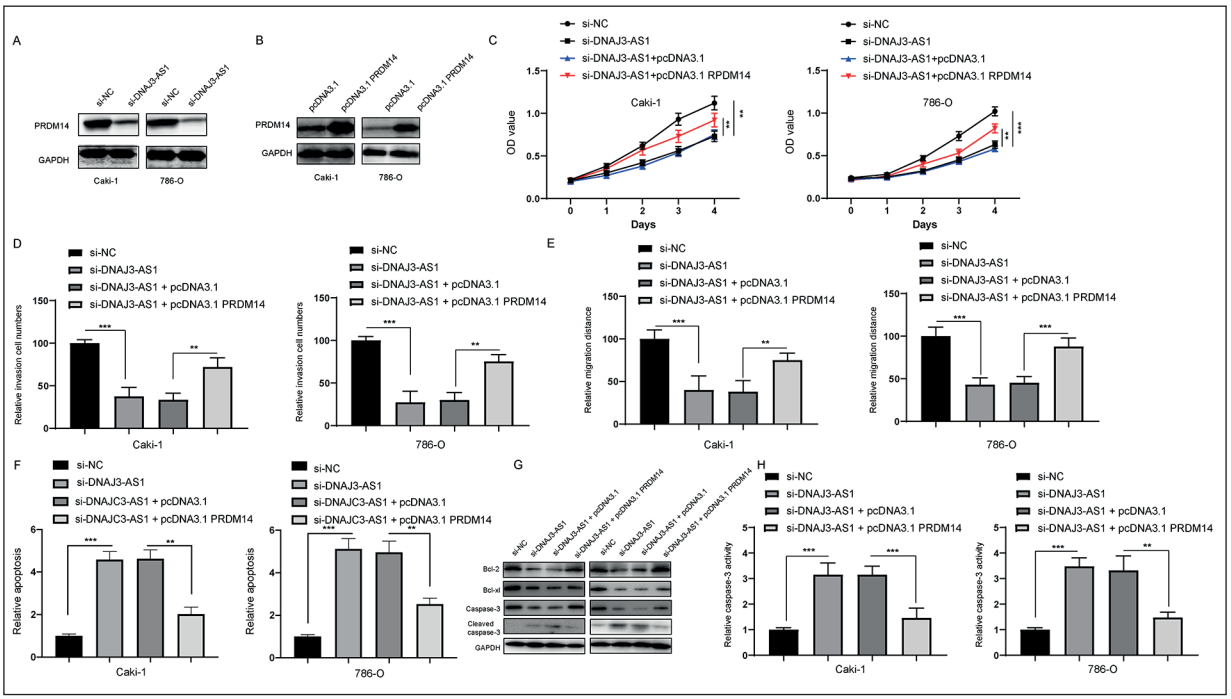

Figure 5. Overexpression of PRDM14 abrogated the effects of silencing of DNAJC3-AS1 in ccRCC cells. **A,** Caki-1 and 786-O cells were transfected with siDNAJC3-AS1 for 24 h, then the protein levels of PRDM14 were measured by Western blot. **B,** Caki-1 and 786-O cells were transfected pcDNA3.1 PRDM14 for 24 h, then protein levels of PRDM14 were measured by Western blot. **C,** Caki-1 and 786-O cells were treated as indicated, then cell proliferation was measured by the CCK-8 assay. **D,** Caki-1 and 786-O cells were treated as indicated, then cell invasion was assayed. **E,** Caki-1 and 786-O cells were treated as indicated, then cell migration was assayed. **F,** Caki-1 and 786-O cells were treated as indicated and then cellular apoptosis was assayed. **G,** Caki-1 and 786-O cells were treated as indicated, indicated proteins were determined by Western blot assay (**H**) Caki-1 and 786-O cells were treated as indicated, the caspase-3 activity was measured. Three independent experiments were performed and data shown are mean ± SD. Statistically significant differences are indicated as **, $p<0.01$, ***, $p<0.001$.

on migration, invasion, and apoptosis were also abrogated by upregulation of PRDM14 (Figure 5D, E, F, G, H). Taken together, these data suggest that DNAJC3-AS1 exerts its oncogenic effects *via* upregulation of PRDM14 in ccRCC cells.

Discussion

The lncRNAs are a group of important newly identified noncoding RNAs that are longer than 200 nucleotides in length. Studies[17-19] indicated that lncRNAs play an essential role in the development of various diseases, such as diabetes mellitus, nervous system disease, and cardiovascular disease. Jiang et al[20] have shown that lncRNAs also play essential roles in the regulation of tumor viability, apoptosis, metastasis, etc. Therefore, lncRNAs have the potential to be used as biomarkers and therapeutic targets for various cancers. In the present study, we showed that the expression level of DNAJC3-AS1 was upregulated in ccRCC samples compared to adjacent normal tissues. Furthermore, we found that high expression of DNAJC3-AS1 was correlated with advanced clinical stage, larger tumor size, more metastasis and advanced pathological grade. Moreover, we also showed that patients with high expression of DNAJC3-AS1 had poorer survival than patients with low expression of DNAJC3-AS1. *In vitro* studies showed that silencing DNAJC3-AS1 suppressed the proliferation, migration and invasion of ccRCC cells. Knockdown of DNAJC3-AS1 also promoted the apoptosis of ccRCC cells. Our findings are in line with a previous study that showed that DNAJC3-AS1 functioned as an oncogene in osteosarcoma[21].

Many studies have highlighted the essential function of lncRNAs as miRNA sponges[22]. In this research, miR-27a-3p was identified to have binding sites complementary to DNAJC3-AS1. The dual-luciferase reporter gene assay verified this finding. Our study showed significant downregulation of miR-27a-3p in ccRCC tis-

sues. Notably, inhibition of miR-27a-3p reversed the regulatory effect of DNAJC3-AS1 on the biological activities of ccRCC cells. Our findings are consistent with a very recent study that showed that miR-27a-3p functions as a tumor suppressor in lung cancer[23]. Zhao et al[24] reported that miR-27a-3p could function as a tumor suppressor via inhibition of the metastasis of liver cancer. It was also found that miR-27a-3p inhibited viability and migration via down-regulation of DUSP16 in hepatocellular carcinoma cells[25]. However, studies have also revealed that miR-27a-3p functions as an oncogene in multiple cancers, such as gastric cancer, osteosarcoma, colorectal cancer and nasopharyngeal carcinoma[26-29]. This discrepancy revealed the complexity of miR-27a-3p in carcinogenesis, and more investigation is needed to unveil more functions of miR-27a-3p.

PRDM14 is a novel transcriptional regulator that has a single PR domain and six tandemly repeated zinc fingers[30]. PRDM14 is involved in multiple cellular functions, such as cellular differentiation, growth, cell cycle distribution and apoptosis[31]. Recently, abnormal expression of PRDM14 has been found in different cancers, such as breast cancer, lung cancer, leukemia and pancreatic cancer[32-34]. Our data revealed high expression of PRDM14 in ccRCC tissues. This finding is in line with previous investigation that reported the oncogenic functions of PRDM14[35]. We hypothesized that DNAJC3-AS1 may regulate PRDM14 by sponging the expression of miR-27a-3p. Our study revealed that silencing PRDM14 inhibited the malignant phenotypes of ccRCC. Moreover, overexpression of PRDM14 reversed the effects of DNAJC3-AS1 silencing on ccRCC cells.

Conclusions

Our data suggested that DNAJC3-AS1 is an oncogene and serves as a ceRNA; this lncRNA together with miR-27a-3p/PRDM14 constitute a signaling pathway that regulates the biological behavior of ccRCC. Therefore, targeting DNAJC3-AS1/miR-27a-3p/PRDM14 may beneficial for the treatment of ccRCC patients and may provide an alternative strategy for ccRCC therapy.

Conflict of Interest

The Authors declare that they have no conflict of interests.

Acknowledgements

This work is supported by Project of Medical Science of Health and Family Planning Bureau of Zhenhai District (No. 2017011, to N.X.Y) and Project of Traditional Chinese Medicine of Zhejiang Province (No. 2019ZA119, to N.X.Y).

References

1) Siegel RL, Miller KD, Jemal A. Cancer statistics, 2019. CA Cancer J Clin 2019; 69: 7-34.
2) Ljungberg B, Campbell SC, Choi HY, Jacqmin D, Lee JE, Weikert S, Kiemeney LA. The epidemiology of renal cell carcinoma. Eur Urol 2011; 60: 615-621.
3) Cech TR, Steitz JA. The noncoding RNA revolution-trashing old rules to forge new ones. Cell 2014; 157: 77-94.
4) Chen Z, Lei T, Chen X, Gu J, Huang J, Lu B, Wang Z. Long non-coding RNA in lung cancer. Clin Chim Acta 2020; 504: 190-200
5) Fattahi S, Kosari-Monfared M, Golpour M, Emami Z, Ghasemiyan M, Nouri M, Akhavan-Niaki H. LncRNAs as potential diagnostic and prognostic biomarkers in gastric cancer: a novel approach to personalized medicine. J Cell Physiol 2020; 235: 3189-3206.
6) Chi Y, Wang D, Wang J, Yu W, Yang J. Long non-coding RNA in the pathogenesis of cancers. Cells 2019; 8.
7) Ye XT, Huang H, Huang WP, Hu WL. LncRNA THOR promotes human renal cell carcinoma cell growth. Biochem Biophys Res Commun 2018; 501: 661-667.
8) Wu Z, Chen D, Wang K, Cao C, Xu X. Long Non-coding RNA SNHG12 functions as a competing endogenous RNA to regulate mdm4 expression by sponging miR-129-5p in clear cell renal cell carcinoma. Front Oncol 2019; 9: 1260.
9) Chen C, Feng Y, Wang X. LncRNA ZEB1-AS1 expression in cancer prognosis: review and meta-analysis. Clin Chim Acta 2018; 484: 265-271.
10) Yang Q, Sun J, Ma Y, Zhao C, Song J. LncRNA DLX6-AS1 promotes laryngeal squamous cell carcinoma growth and invasion through regulating miR-376c. Am J Transl Res 2019; 11: 7009-7017.
11) Gong CY, Tang R, Liu KX, Xiang G, Zhang HH. Long non-coding RNA TP73-AS1 in cancers. Clin Chim Acta 2020; 503: 151-156.
12) Synofzik M, Haack TB, Kopajtich R, Gorza M, Rapaport D, Greiner M, Schönfeld C, Freiberg C, Schorr S, Holl RW, Gonzalez MA, Fritsche A, Fallier-Becker P, Zimmermann R, Strom TM, Meitinger T, Züchner S, Schüle R, Schöls L, Prokisch H. Absence of BiP co-chaperone DNAJC3 causes diabetes mellitus and multisystemic neurodegeneration. Am J Hum Genet 2014; 95: 689-697.
13) Petrova K, Oyadomari S, Hendershot LM, Ron D. Regulated association of misfolded endoplas-

mic reticulum lumenal proteins with P58/DNAJc3. EMBO J 2008; 27: 2862-2872.

14) Martínez-Salamanca JI, Huang WC, Millán I, Bertini R, Bianco FJ, Carballido JA, Ciancio G, Hernández C, Herranz F, Haferkamp A, Hohenfellner M, Hu B, Koppie T, Martínez-Ballesteros C, Montorsi F, Palou J, Pontes JE, Russo P, Terrone C, Villavicencio H, Volpe A, Libertino JA; International Renal Cell Carcinoma-Venous Thrombus Consortium. Prognostic impact of the 2009 UICC/AJCC TNM staging system for renal cell carcinoma with venous extension. Eur Urol 2011; 59: 120-127.
15) Yu R, Yu BX, Chen JF, Lv XY, Yan ZJ, Cheng Y, Ma Q. Anti-tumor effects of atractylenolide I on bladder cancer cells. J Exp Clin Cancer Res 2016; 35: 40.
16) Bartel DP. MicroRNAs: genomics, biogenesis, mechanism, and function. Cell 2004; 116: 281-297.
17) Yan Y, Song D, Song X, Song C. The role of lncRNA MALAT1 in cardiovascular disease. IUBMB Life 2020; 72: 334-342.
18) Guo J, Liu Z, Gong, R. Long noncoding RNA: an emerging player in diabetes and diabetic kidney disease. Clin Sci (Lond) 2019; 133: 1321-1339.
19) Kopp F. Molecular functions and biological roles of long non-coding RNAs in human physiology and disease. J Gene Med 2019; 21: e3104.
20) Jiang MC, Ni JJ, Cui WY, Wang BY, Zhuo W. Emerging roles of lncRNA in cancer and therapeutic opportunities. Am J Cancer Res 2019; 9: 1354-1366.
21) Liang R, Liu Z, Chen Z, Yang Y, Li Y, Cui Z, Chen A, Long Z, Chen J, Lu J, Huang B, Li Q. Long noncoding RNA DNAJC3-AS1 promotes osteosarcoma progression via its sense-cognate gene DNAJC3. Cancer Med 2019; 8: 761-772.
22) Paraskevopoulou MD, Hatzigeorgiou AG. Analyzing miRNA-LncRNA interactions. Methods Mol Biol 2016; 1402: 271-286.
23) Yan X, Yu H, Liu Y, Hou J, Yang Q, Zhao Y. MiR-27a-3p functions as a tumor suppressor and regulates non-small cell lung cancer cell proliferation via targeting HOXB8. Technol Cancer Res Treat 2019; 18: 1533033819861971.
24) Zhao N, Sun H, Sun B, Zhu D, Zhao X, Wang Y, Gu Q, Dong X, Liu F, Zhang Y, Li X. miR-27a-3p suppresses tumor metastasis and VM by down-regulating VE-cadherin expression and inhibiting EMT: an essential role for Twist-1 in HCC. Sci Rep 2016; 6: 23091.
25) Li JM, Zhou J, Xu Z, Huang HJ, Chen MJ, Ji JS. MicroRNA-27a-3p inhibits cell viability and migration through down-regulating DUSP16 in hepatocellular carcinoma. J Cell Biochem 2018; 11: 5143-5152.
26) Zhou L, Liang X, Zhang L, Yang L, Nagao N, Wu H, Liu C, Lin S, Cai G, Liu J. MiR-27a-3p functions as an oncogene in gastric cancer by targeting BTG2. Oncotarget 2016; 7: 51943-51954.
27) Liu J, Li M, Liu X, Liu F, Zhu J. MiR-27a-3p promotes the malignant phenotypes of osteosarcoma by targeting ten-eleven translocation 1. Int J Oncol 2018; 52: 1295-1304.
28) Liang J, Tang J, Shi H, Li H, Zhen T, Duan J, Kang L, Zhang F, Dong Y, Han A. MiR-27a-3p targeting RXRalpha promotes colorectal cancer progression by activating Wnt/beta-catenin pathway. Oncotarget 2017; 8: 82991-83008.
29) Li L, Luo Z. Dysregulated miR-27a-3p promotes nasopharyngeal carcinoma cell proliferation and migration by targeting Mapk10. Oncol Rep 2017; 37: 2679-2687.
30) Nakaki F, Saitou M. PRDM14: a unique regulator for pluripotency and epigenetic reprogramming. Trends Biochem Sci 2014; 39: 289-298.
31) Taniguchi H. and Imai K. Silencing PRDM14 via oligonucleotide therapeutics suppresses tumorigenicity and metastasis of breast cancer. Methods Mol Biol 2019; 1974: 233-243.
32) Nishikawa N, Toyota M, Suzuki H, Honma T, Fujikane T, Ohmura T, Nishidate T, Ohe-Toyota M, Maruyama R, Sonoda T, Sasaki Y, Urano T, Imai K, Hirata K, Tokino T. Gene amplification and overexpression of PRDM14 in breast cancers. Cancer Res 2007; 67: 9649-9657.
33) Zhang T, Meng L, Dong W, Shen H, Zhang S, Liu Q, Du J. High expression of PRDM14 correlates with cell differentiation and is a novel prognostic marker in resected non-small cell lung cancer. Med Oncol 2013; 30: 605.
34) Dettman EJ, Simko SJ, Ayanga B, Carofino BL, Margolin JF, Morse HC 3rd, Justice MJ. Prdm14 initiates lymphoblastic leukemia after expanding a population of cells resembling common lymphoid progenitors. Oncogene 2011; 30: 2859-2873.